Bio-Design and Manufacturing (2022) 5:153–162
https://doi.org/10.1007/s42242-021-00143-6

RESEARCH ARTICLE

Preparation of conductive and transparent dipeptide hydrogels for wearable biosensor

Yafeng Jing[1] · Anhe Wang[2] · Jieling Li[2] · Qi Li[2] · Qingquan Han[2] · Xuefang Zheng[3] · Hongyu Cao[1,3] · Shuo Bai[2]

Received: 4 March 2021 / Accepted: 8 June 2021 / Published online: 8 July 2021

Abstract

Conductive and transparent dipeptide hydrogels are desirable building blocks to prepare soft electronic devices and wearable biosensors due to their excellent biocompatibility, multi-functionality, and physiochemical properties similar to those of body tissues. However, the preparation of such hydrogels featuring high conductivity and transparency is a huge challenge because of the hydrophobic feature of conductive additives making the doping process difficult. To overcome this issue, hydrophilic conductive polydopamine (PDA)-doped polypyrrole (PPy) nanoparticles are introduced into the dipeptide hydrogel networks to form conductive nanofibrils *in situ* to achieve a good level of hydrophilic templating of the hydrogel networks. This technique creates a complete conductive network and allows visible light to pass through. The strategy proposed herein not only endows the dipeptide hydrogel with good conductivity and high transparency, but also provides a great potential application of conductive dipeptide hydrogels for body-adhered signal detection, as evidenced by the experimental data.

Keywords Conductivity · Transparency · Peptide hydrogel · Polypyrrole-polydopamine nanoparticles · Wearable biosensor

Introduction

Hydrogels with high conductivity and transparency have promising potential applications in wearable devices, especially as building blocks to fabricate biosensors that can integrate with the human body to assay physiological parameters in real time [1–5]. Until now, most proposed conductive hydrogels were opaque as they were doped with high levels of nontransparent conductive nanoparticles, such as metal-based (Au, Ag) nanowires or nanoparticles [6, 7], carbon-based nanomaterials (carbon nanotube, graphene) [8, 9], and conductive polymer-based nanoparticles [polypyrrole (PPy), polyaniline (PI), and poly(3,4-ethylenedioxythiophene) (PEDOT)] [10–12]. Nevertheless, the transparency of conductive hydrogels is a significant requirement for biosensors to satisfy the needs of translucent data recording and operations [13–15]. This challenge was addressed by proposing polymer networks with ionic liquids and the preparation of a transparent and conductive hydrogel. The possibility of ionic liquid leakage from hydrogels, especially in physiological environments, however, is a potential threat to human health, limiting the application of such polymer networks in the field of wearable biosensors [16, 17]. In a different approach, conductive polymers were employed to fabricate nanostructures sized less than half the shortest wavelength of visible light, which are introduced into the network of hydrogels as nanofillers [10–12]. Unfortunately, these nanostructures suffer from aggregation during the process of hydrogel fabrication, resulting in decreased conductivity. The phenomenon is caused by the hydrophobic feature of conductive polymers making them insoluble and mismatch with the hydrophilic fibers of hydrogels. Recently, Lu's group developed PPy nanoparticles functionalized by polydopamine (DPA) (denoted as PPy@PDA) to improve

Yafeng Jing and Anhe Wang have contributed equally to this work.

✉ Anhe Wang
ahwang@ipe.ac.cn

✉ Hongyu Cao
caohongyu@foxmail.com

✉ Shuo Bai
baishuo@ipe.ac.cn

[1] College of Life Science and Biotechnology, Dalian University, Dalian 116622, China

[2] State Key Laboratory of Biochemical Engineering, Institute of Process Engineering, Chinese Academy of Sciences, Beijing 100190, China

[3] College of Environmental and Chemical Engineering, Dalian University, Dalian 116622, China

the hydrophilic properties and used them as nanofillers to fabricate hydrogels [18]. The proposed strategy overcomes very well the mismatching between the hydrophobicity of nanofillers and the hydrophilicity of hydrogel matrix. During the hydrogel preparation process, the ammonium persulfate (APS) not only plays the role of initiator to polymerize monomer acrylamide to form hydrogels, but also induces the PPy@PDA to transform from nanoparticles to nanofibrils templating on polyacrylamide hydrogel chains. The prepared hydrogels show excellent features of high conductivity, transparency, and adhesiveness. However, the residual monomer acrylamide overshadows their application in wearable devices, which needs to be removed from hydrogel by soaking to eliminate its toxicity [19, 20]. Therefore, it is necessary to develop new biocompatible, transparent and conductive hydrogel materials to meet the safety requirements of wearable devices.

Peptides as biocompatible, bioactive, and biodegradable compounds play a crucial role in the construction of functional hydrogels and have wide potential applications in biomedicine such as tissue engineering, catalysis, drug encapsulation and release [21–23]. Especially, the dipeptides and derivatives with definite chemical structures and specific self-assembling features, which can be designed at the molecular level and synthesized on a large scale, are ideal building blocks to prepare hydrogels with controlled physicochemical properties by changing the self-assembly conditions (enzyme, pH, temperature, ionic concentration, etc.) [22, 24–27]. Under certain conditions, the dipeptides will self-assemble into various nanostructures (nanofiber, nanobelt, etc.) and cross-link to form hydrogels through reversible intermolecular weak interactions, such as hydrogen bonds, van der Waals forces, hydrophobic, electrostatic and π–π stacking interactions [24–27]. Therefore, such flexible assembly behaviors of dipeptides are favored for the fabrication of conductive and transparent hydrogels, because the surface properties (hydrophilicity and hydrophobicity) of fibers of dipeptide hydrogels can be altered by selecting the suitable molecular sequences and intermolecular weak interactions.

In this work, an enzyme-catalyzed peptide self-assembly strategy is proposed to prepare dipeptide hydrogels with good conductivity and transparency. During the experimental process, thermolysin was used as a catalyst to promote the condensation reactions of Fmoc-tyrosine-OH (Fmoc-Y), Fmoc-leucine-OH (Fmoc-L), Fmoc-threonine-OH (Fmoc-T) and Fmoc-serine-OH (Fmoc-S) with H-leucine-NH_2 (L-NH_2), forming dipeptide hydrogels with tunable physicochemical properties [26, 28, 29]. Meanwhile, hydrophilic conductive PPy@PDA nanofillers were introduced into the hydrogel network templates to form conductive nanofibrils, as shown in Scheme 1. This technique confers the dipeptide hydrogels good conductivity, transparency and provides a great potential application value in biosensors to precisely record tiny movements of the human body.

Materials and methods

Materials

Fmoc-Y, Fmoc-L, thermolysin enzyme, polyvinyl alcohol (PVA, Mw 10000), pyrrole, and dopamine were purchased from Sigma-Aldrich, the USA. Fmoc-S and APS for

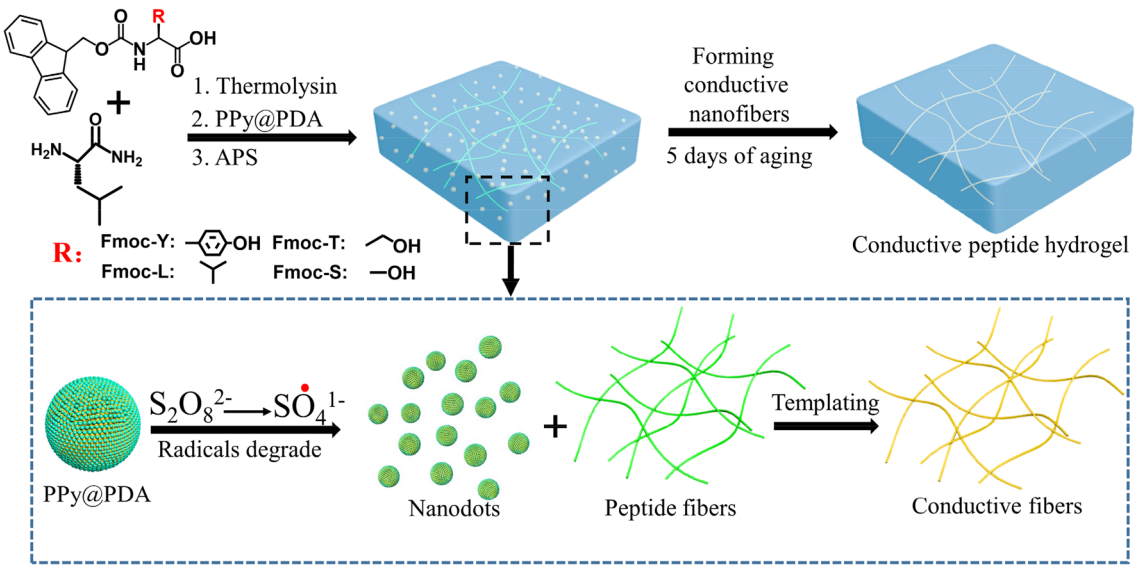

Scheme 1. Process and mechanism of transparent and conductive dipeptide hydrogel preparation

electrophoresis were obtained from J&K Chemicals, Shanghai, China. Fmoc-T and L-NH_2 were obtained from Bachem, Tübinge, Germany. Hoechst 33342 and Alexa Fluor 488 dyes were acquired from Molecular Probes Inc., the USA, and all other reagents were obtained from Beijing Chemical Reagent Co., Beijing, China. The water was purified by a Milli-Q@IQ 7003 system from Millipore Co., the USA. All required chemicals were used without further purification.

Methods

Fabrication of PPy@PDA nanoparticles

Hydrophilic PPy@PDA nanoparticles were prepared based on the method proposed by Lu's group with some modifications [18]. Firstly, PVA (3.0 g, Mw 10000) was dissolved in 40 mL deionized water and heated to 90 °C with magnetic stirring. After the complete dissolution of PVA, the solution was cooled to room temperature. Subsequently, pyrrole monomer (4 mmol, 280 μL) and dopamine monomer (0.1 g) were separately added into 5 mL PVA solution each, and the mixtures were vigorous shaken. Next, $FeCl_3{\cdot}6H_2O$ (9.2 mmol, 2.4 g) was dissolved into the remaining PVA solution (35 mL) and transferred to a 0 °C water bath. Finally, the pyrrole and dopamine monomer solutions were added to the $FeCl_3$ solution, which was continually stirred in a 0 °C bath for 9 h until the polymerization of monomers was complete. The obtained final product was washed with hot water three times to remove impurities and was stored at 4 °C until further use.

Preparation of conductive dipeptide hydrogel

Fmoc-Y/L/T/S (30 mmol/L) and L-NH_2 (120 mmol/L) were dissolved in 1 mL phosphate buffer solution (PBS, pH 8.0, 0.1 mol/L), and the mixture was vigorously shaken. Next, 0.5 mg PPy@PDA nanoparticles and 20 mg APS were dissolved in 300 μL deionized water, and the latter was added to the above substrate solution. Finally, enzyme thermolysin (1 mg) was added to the mixture accompanied by vigorous shaking. The obtained hydrogels were stored at room temperature for 9 d.

Rheological properties of samples

A rheometer (Anton Paar MCR302) with a 12-mm-diameter parallel plate (PP12) was utilized to measure the rheological properties of samples at pre-determined times. The amplitude sweep was conducted at a shear-strain (γ) range of 0.01% to 1000% and 1 Hz frequency, and the relationship between the storage modulus and the loss modulus of the sample was recorded.

Conductivity of peptide hydrogels

Samples were prepared with a square shape of 1.2 cm × 1.2 cm × 0.25 cm. The corresponding conductivity of samples was measured by the RTS-8 four-probe test system equipped with an RTS-9 double electric four-probe tester (Guangzhou Four Probe Electronic Technology Co., Ltd., China). The average distance between probes and samples was 1.59 mm, and the current was 0.7373 mA.

Transmittance of peptide hydrogels

Samples with 2 mm thickness were placed on a quartz substrate with a size of 0.8 cm × 2.0 cm, and the visible absorption spectrum in the range of 400–800 nm was measured by a Shimadzu UV-2600 spectrophotometer (Shimadzu, Japan).

Cytotoxicity in vitro

Firstly, C2C12 cells (Mouse myoblast cell) were cultured in 96-well plate overnight to allow cell adhesion. The cells were then incubated with different concentrations of dipeptide hydrogels (1, 2, 5, 8, 10, 20 mg/mL) for 24 h, and cell viability was detected by the CCK8 method.

Biocompatibility of dipeptide hydrogels

Dipeptide hydrogels with 1 mm thickness and 3.5 mm diameter were prepared in a Petri dish. Next, C2C12 cells were added to the surface of samples for co-incubation for 16 h. Finally, the nuclei and membrane of cells were stained with Hoechst 33342 (50 μg/mL, Molecular Probes Inc., the USA) and Alexa Fluor 488 (50 μg/mL) to observe cell morphology by a Leica SP-8 laser confocal microscope.

Motion signals recorded by dipeptide hydrogel sensor

The motion sensors were attached to the finger joint, wrist joint, and elbow joint, separately. Subsequently, the sensors were connected to the electrochemical workstation (CH Instrument, Inc., China) to record the change of current with the software of the Amperometric *i-t* Curve system. The voltage was fixed as 0.1 V, and the sampling interval was set as 0.1 or 0.2 s.

Characterization and equipment

The morphology and structure of dipeptide hydrogels were investigated by scanning electron microscopy (SEM, HITACHI S-4800, Japan) and transmission electron microscopy (TEM, JEOL-JEM-2100, Japan). FTIR spectra were recorded by the FTIR spectrometer system (6800 FTIR, Beijing, China). The HITACHI S-4800 EDX system was

applied to detect the element change of dipeptide hydrogels during the aging process. The secondary structure of samples was determined by a J-810 circular dichroism spectrometer (CD, JASCO, Tokyo, Japan). The Agilent 1260 Infinity II high-performance liquid chromatography system equipped with an Agilent Poroshell 120 EC-C18 column of 150 mm length, 3.0 mm internal diameter, and 2.7 μm particle size was used to quantify the conversion efficiency through the measurement of enzyme catalytic activity.

Results and discussion

Preparation of PPy@PDA nanoparticles and dipeptide hydrogels

PPy is an excellent conductive polymer that has been widely applied to prepare functional materials in the fields of wearable devices and biosensors [13, 30]. However, PPy nanofillers suffer from poor dispersibility in an aqueous solution due to their strong hydrophobicity, resulting in the aggregation of nanofillers and subsequent low conductivity of the formed materials in further applications. In order to improve the hydrophilicity of PPy nanofillers, PDA, a popular agent in surface modification was introduced in the preparation process of PPy because of its abundant functional groups, such as carboxyl, amino, imine, and phenol groups [31, 32].

PDA-doped PPy nanoparticles with good hydrophilicity were fabricated under mild conditions where $FeCl_3$ was used as an oxidant [18]. As shown in Fig. 1a, PPy@PDA nanoparticles had an average size of about 150–300 nm and displayed a good dispersibility in aqueous solution (Fig. S1a). In addition, the TEM image also showed a result similar to that of SEM (Fig. 1b), which indicated the successful fabrication of PPy@PDA nanofillers. In our previous work [26, 28, 29], enzyme thermolysin as an initiator could catalyze condensation reactions between Fmoc-Y, -L, -T, -S and L-NH_2 to form transparent dipeptide hydrogels with high efficiency (Fig. S1b, the formed dipeptides are denoted as Fmoc-YL, Fmoc-LL, Fmoc-TL, and Fmoc-SL, respectively). Herein, PPy@PDA nanoparticles as nanofillers were introduced into the above reaction to prepare transparent and conductive dipeptide hydrogels, in which the fibers of hydrogels could be taken as templates to direct the formation of conductive nanofibrils. As shown in Fig. 1c, dipeptide hydrogels with PPy@PDA nanoparticles were obtained immediately after the addition of enzyme. Meanwhile, photographs showed that four obtained hydrogels had a brown black color following the addition of PPy@PDA nanoparticles (1.1%, wt%), which became light brown yellow after 5 d of aging. It should be noted that the transparency of four hydrogel samples was improved compared with the initial samples (Fig. 1c). When the hydrogels had 2 mm thickness, four samples exhibited good transparency values (> 70% across the visible spectrum, Figs. 1d and S2) [18]. Moreover, high-performance chromatography was carried out to assay the conversion efficiency of condensation reactions (Fig. S3), which yielded values of 76.5%, 83.25%, 56.6%, and 51.6% for Fmoc-YL, Fmoc-LL, Fmoc-TL, and Fmoc-SL, respectively.

Physicochemical properties of dipeptide hydrogels

In order to study the morphological change of four hydrogels with PPy@PDA nanoparticles during the aging process, samples at a pre-determined time point were collected and assayed by SEM as shown in Fig. 2a. The PPy@PDA nanoparticles and hydrogel fibers could be clearly observed on the first day after mixing the nanoparticles with hydrogels. Interestingly, after 5 d of aging, the nanoparticles

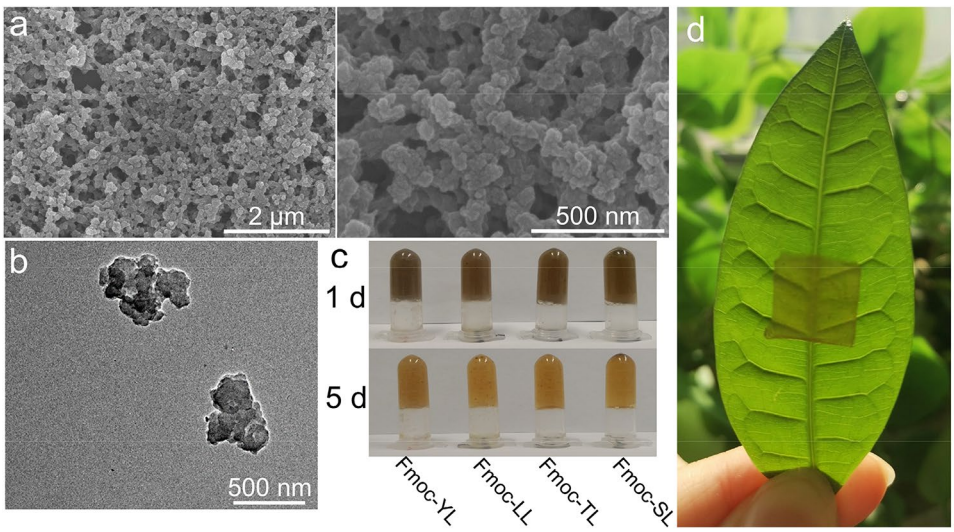

Fig. 1 Morphology of PPy@PDA nanoparticles by **a** SEM and **b** TEM; **c** photograph of transparency change of dipeptide hydrogels with PPy@PDA nanoparticles during the aging process; **d** representative photograph of the transparent hydrogel covering on a leaf

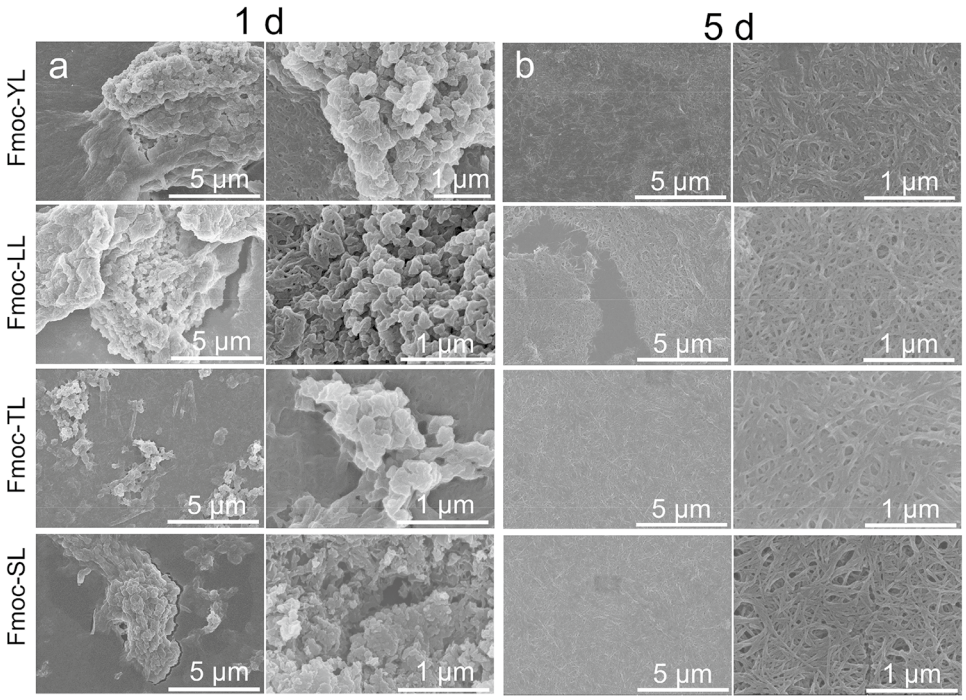

Fig. 2 SEM images of morphological changes in dipeptide hydrogels with PPy@PDA nanoparticles during the aging process after **a** 1 d and **b** 5 d

disappeared and only fibers could be seen. Compared with hydrogels without PPy@PDA nanoparticles (Fig. S4), no obvious changes were observed in fibers of the hydrogel networks, which had a length of about several micrometer and a diameter of about 20–50 nm. It is assumed that the transparency improvement of hydrogels could be ascribed to the conversion of PPy@PDA nanofillers from nanoparticles to conductive nanofibrils, which took the hydrogel fibers as templates. During the aging process (Scheme 1), free radicals derived from APS continuously eradicated π–π stacking interactions between the oligomeric units in the PPy@PDA nanoparticles, resulting in nanodots which could self-assemble to form conductive nanofibrils guided by dipeptide hydrogel fibers [18]. EDX experiments were also performed to detect the composition change in four hydrogel samples. The content of N in Fmoc-YL hydrogels increased from 6.18% (wt%) to 12.65% (wt%) after the addition of PPy@PDA nanoparticles (Fig. 3), which strongly demonstrated the successful formation of conductive nanofibrils in Fmoc-YL hydrogel networks. Moreover, the other three kinds of dipeptide hydrogels displayed similar results (Fig. S6).

Next, the rheological properties were also investigated. As shown in Fig. 4a and 4b, the storage moduli (G') of all hydrogels surpassed the corresponding loss moduli (G'') by almost one order of magnitude indicating accordant gel states. Meanwhile, the hydrogels with PPy@PDA nanoparticles showed higher storage moduli than these without nanofillers on the first day, which can be attributed to the reinforcement effect of fillers within hydrogel networks [33]. However, during the aging process, the

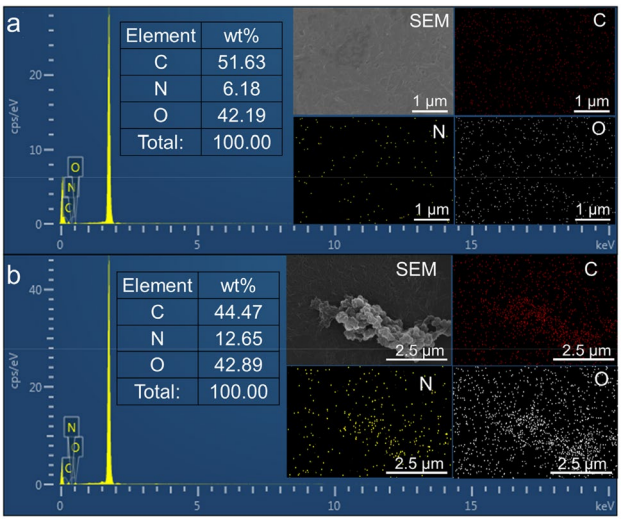

Fig. 3 EDX spectra of dipeptide hydrogels **a** without and **b** with PPy@PDA nanoparticles after 5 d of aging

storage moduli of hydrogels with nanofillers displayed a decreasing tendency. This can be explained by the fact that nanodots detached from PPy@PDA nanoparticles by APS interfered and involved in the self-assembly of dipeptide molecules [18]. Among the four hydrogels with nanofillers, the Fmoc-YL hydrogel possessed the strongest storage modulus [(10.7 ± 0.2) kPa] compared to that of Fmoc-LL [(2.7 ± 0.1) kPa], Fmoc-TL [(2.6 ± 0.1) kPa], and Fmoc-SL [(1.4 ± 0.1) kPa] after 5 d of aging (Fig. 4b bottom).

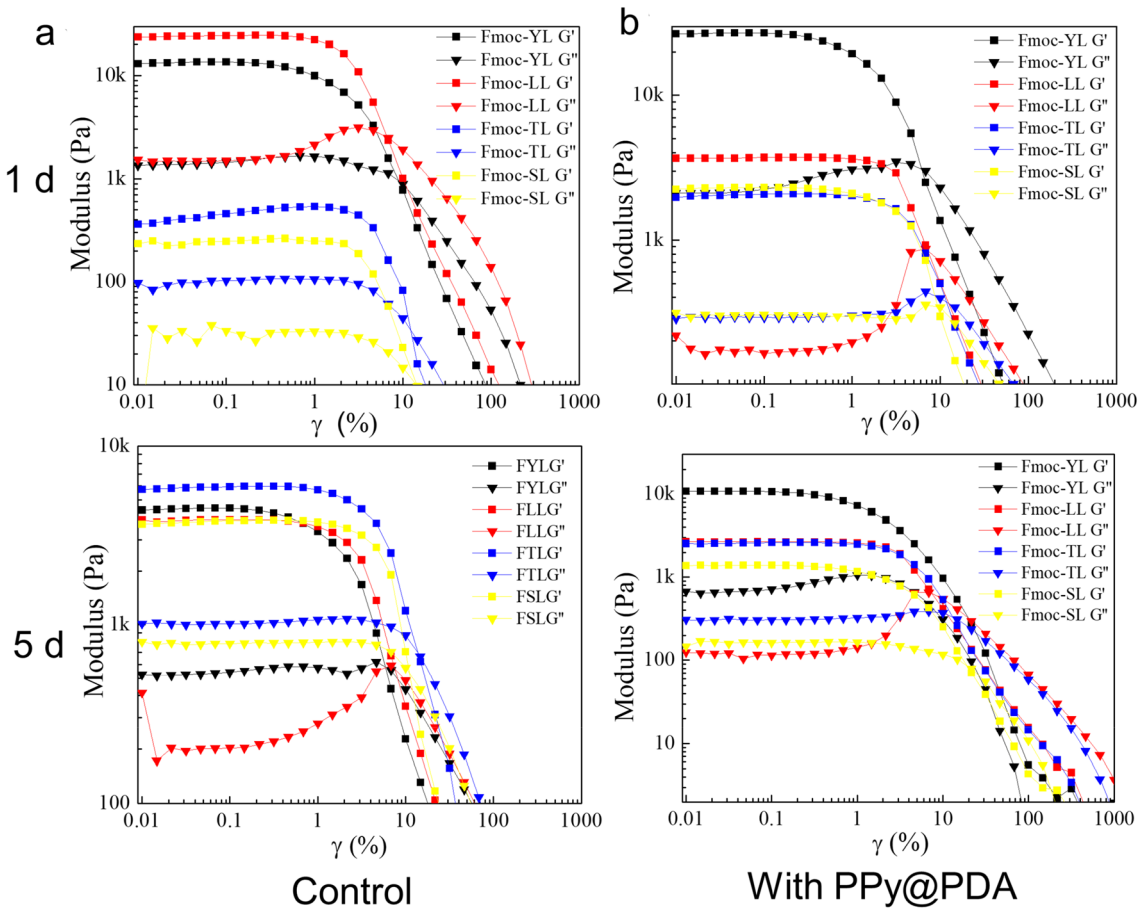

Fig. 4 Variation of rheological properties of dipeptide hydrogels **a** without and **b** with PPy@PDA nanoparticles after 1 d and 5 d aging

FTIR was also performed to measure the compositional changes during the aging process. As shown in Fig. 5a, characteristic bands of PPy ascribed to the C–H in-plane deformation vibration (1045 cm^{-1}), C–C asymmetric stretching vibration (1450 cm^{-1}), and ring-stretching mode of Py ring (1540 cm^{-1}) could be clearly found in the profile compared with those without PPy@PDA nanofillers (Fig. S5) [34]. Meanwhile, no obvious change in FIIR was observed after 5 d of aging (Fig. 5a bottom).

The CD data in Fig. 5b display the chirality variation of fibers in the hydrogel networks with PPy@PDA nanofillers during the aging process. On the first day, a positive peak appeared at 191 nm and a negative peak at 206 nm for the formed fibers of Fmoc-YL, illustrating the predominantly antiparallel β-sheet secondary structure (black trace, Fig. 5b) [26, 35]. However, the secondary structure of Fmoc-LL fibers displayed a random coil with negative peaks at 200 nm and 235 nm, and a positive peak at 216 nm (red trace, Fig. 5b) [36]. For Fmoc-TL fibers (blue trace, Fig. 5b), an α-helix secondary structure could be detected with a positive peak at 191 nm and negative peaks at 206 nm and 235 nm [37]. Furthermore, a β-turn secondary structure could be attributed to Fmoc-SL fibers, which showed negative peaks at 195 nm and 233 nm and a positive peak at 209 nm (blackish green trace, Fig. 5b) [38]. After 5 d aging, no obvious changes in the secondary structure of the CD profile were observed, as shown in Fig. 5b (bottom).

Biocompatibility and conductivity of dipeptide hydrogel biosensor

The biocompatibility of materials is a significant characteristic in the field of wearable devices that come to direct contact with the human body [39]. Peptide-based materials have excellent biocompatibility and are non-toxic to cells [25–27]. Herein, the four hydrogel samples with PPy@PDA nanoparticles at different concentrations were incubated with C2C12 cells to assay the toxicity of hydrogels. No hydrogels showed any obvious effect on the viability of cells up to the concentration of 10 mg/mL, indicating their excellent safety (Fig. 6a). At the same time, the confocal laser scanning microscopy (CLSM) images (Fig. 6b) displayed that cells could adhere to and spread on the surface of hydrogels, while no dead cells were found.

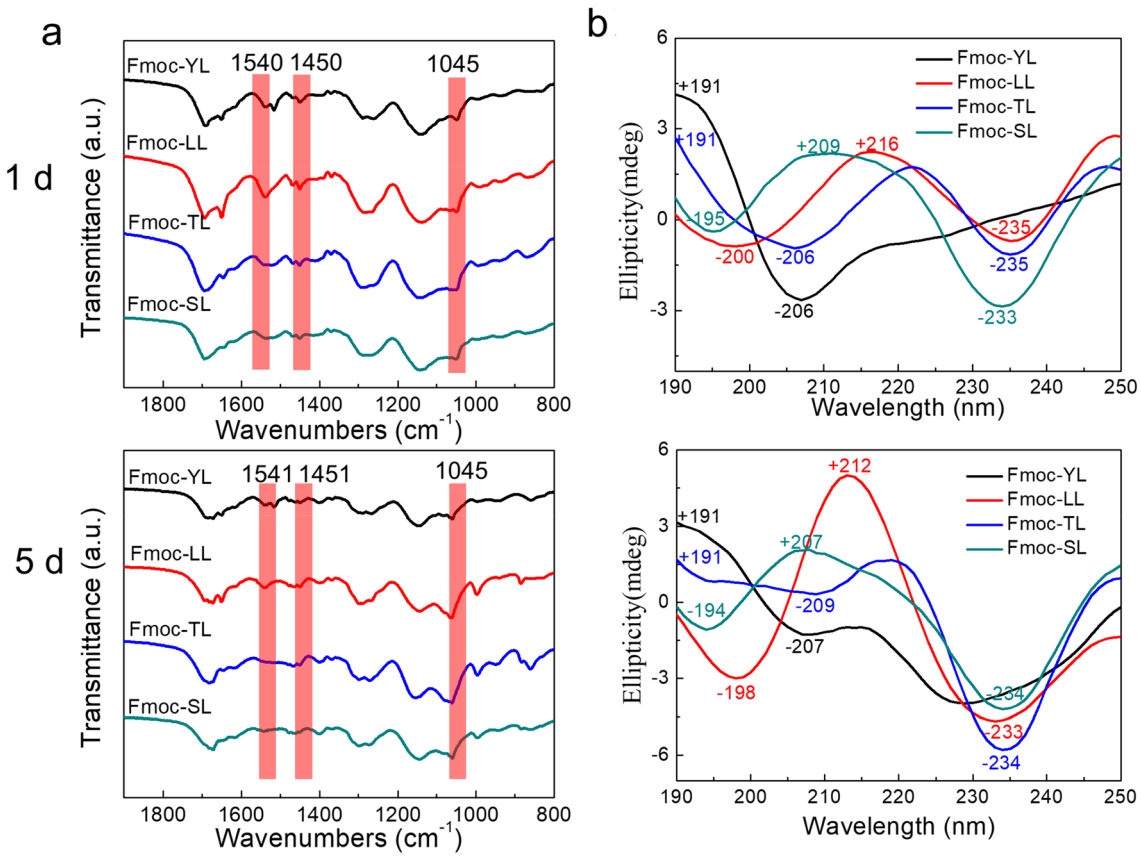

Fig. 5 Changes in the FTIR (**a**) and CD (**b**) spectra of dipeptide hydrogels with PPy@PDA nanoparticles after 1 d and 5 d aging

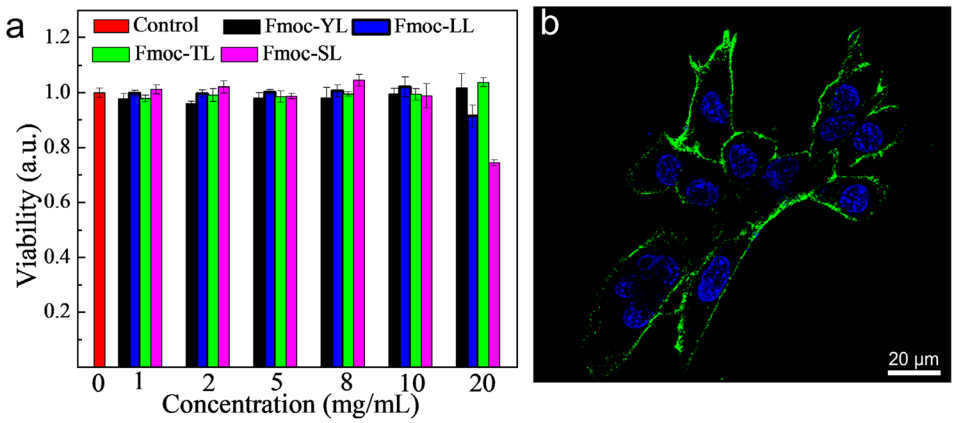

Fig. 6 **a** Toxicity of transparent and conductive dipeptide hydrogels to C2C12 cells; **b** CLSM image of representative biocompatibility of Fmoc-YL hydrogels with PPy@PDA nanoparticles

In the next step, the changes in conductivity of the four hydrogel samples were assessed during the aging process. As shown in Figs. 7a and S7, conductivity could be improved significantly and continuously by PPy@PDA nanoparticles with aging time compared with those without nanoparticles, with no change in conductivity occurring in the latter (Figs. 7a and S8). It is considered that this continuous improvement could be ascribed to the gradual formation of conductive fibers crossing the hydrogel networks. Among the four samples, the Fmoc-LL hydrogel possessed the highest conductivity of about 0.03 S/cm, which was twice as high as that of hydrogel without PPy@PDA nanoparticles. It was assumed that the highly hydrophobic side chains of Fmoc-LL fibers benefited the self-assembly of nanodots that detached from PPy@PDA nanoparticles. Although PPy was doped with hydrophilic PDA molecules,

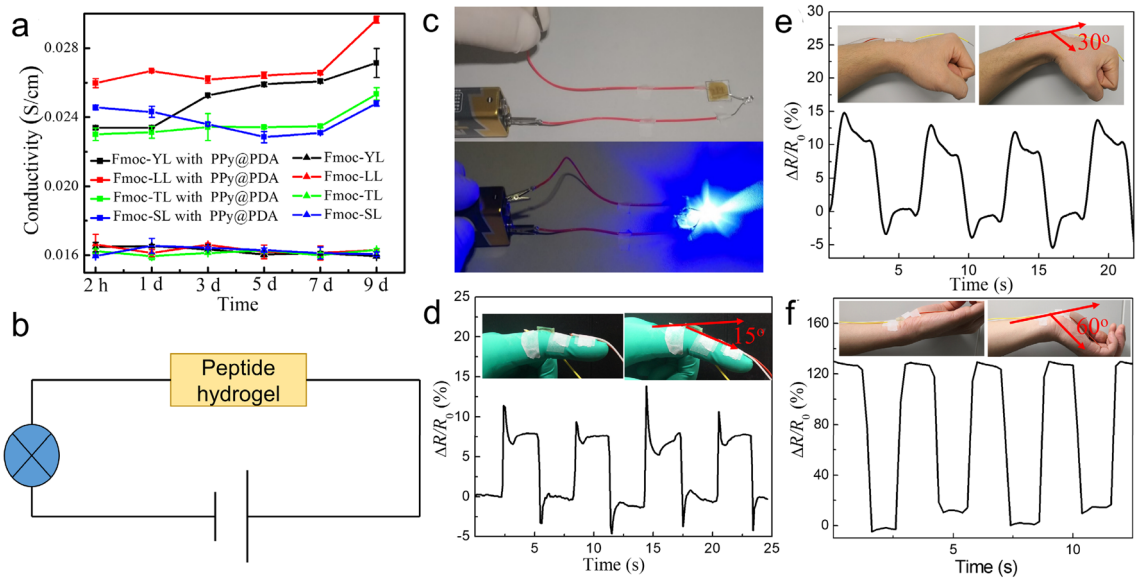

Fig. 7 **a** Variation in the conductivity of dipeptide hydrogels with and without PPy@PDA nanoparticles during 9 d of aging; **b** schematic illustration of designed circuit with LED light; **c** photographs of the circuit based on Fmoc-YL hydrogels with PPy@PDA nanoparticles. Detection of joint motion with different bending angles by conductive Fmoc-LL hydrogel-based sensor: **d** 15°; **e** 30°; **f** 60°

it favored hydrophobic side chains to guide the self-assembly [18]. Moreover, to exclude the possibility that the addition of PPy@PDA nanofillers could also improve the conductivity of hydrogels, APS was excluded from the reaction systems, as depicted in Fig. S9. The four hydrogel samples showed similar conductivity with those without PPy@PDA nanofillers, which could be explained by the lack of produced free radicals to accelerate the conversion of nanofillers from nanoparticles to conductive nanofibrils. Furthermore, conductive assaying illustrated that the other three hydrogels (Fmoc-YL, Fmoc-TL, and Fmoc-SL) with nanofillers featured conductivity in the range of 0.025–0.027 S/cm, meaning that dipeptide hydrogels with tunable conductivities could be prepared by selecting different peptide sequences.

In order to demonstrate the potential application of conductive hydrogels in the field of manufacturing wearable electronics, a simple circuit with an LED light was designed and built, as shown in Fig. 7b and 7c. It was observed that the LED light was instantaneously on after connecting the circuit (voltage, 3 V, Fig. 7c), indicating the excellent conductivity of dipeptide hydrogels (Fmoc-LL) with nanofillers. On the contrary, the LED emitted only weak light under the same conditions when hydrogels without PPy@PDA were applied to build the circuit (Fig. S10).

In the following experiments, a motion sensor formed by Fmoc-LL hydrogels with nanofillers was constructed and used to record the relationship between resistance and different bending angles. As depicted in Fig. 7d–7f, a regular relative change of resistance ($\Delta R/R_0$, where ΔR is the resistance at different bending angles, and R_0 is the resistance at a bending angle of 0°) was observed at different bending angles (15°, 30°, and 60°), which indicated a stable and repeatable change of resistance during the bending experiments. For example, when the bending angle was 15°, the $\Delta R/R_0$ could reach a value about 7, showing excellent signal/noise ratio and repeatability. Meanwhile, when the bending angles were increased from 30° to 60°, the value of $\Delta R/R_0$ changed accordingly. Therefore, the sensor could be employed to accurately assay motions of the human body.

Conclusions

In this paper, transparent and conductive dipeptide hydrogels were fabricated by the doping of PPy@PDA nanofillers. During the preparation process, thermolysin was utilized as a catalyst to initiate condensation reactions between Fmoc-Y, Fmoc-L, Fmoc-T, Fmoc-S, and L-NH_2. The obtained dipeptides could self-assemble into a fibrous network and form stable hydrogels, which were used as an excellent template to guide the formation of conductive nanofibrils through the catalyzing effect of APS. Experiment data showed that the four conductive hydrogels possess high transmittance across the visible spectrum (> 70%, thickness, 2 mm). Meanwhile, the fabricated hydrogels display excellent conductivity that can be altered by the selection of peptide sequences. In addition, cell experiments demonstrated that the four hydrogels have good biocompatibility even up to a hydrogel concentration of 10 mg/mL. Moreover, the hydrogels applied in the construction of a motion senor can precisely assay the

change of bending angles of human joints through the alteration of relative resistance and do so with high stability and repeatability. Therefore, the proposed highly biocompatible, transparent, and conductive hydrogels have wide potential applications in the field of biosensors.

Supplementary Information The online version contains supplementary material available at https://doi.org/10.1007/s42242-021-00143-6.

Acknowledgements The authors acknowledge financial support from the Beijing Municipal Natural Science Foundation (No. 7212206), the National Natural Science Foundation of China (Nos. 21774132, 22072155, 22002170, 21571025, and 21601025), and Project of Young Science and Technology Star of Dalian (No. 2017RQ156).

Author contributions SB, AHW, and HYC contributed to supervision and review & editing. YFJ, JLL, QL, and QQH performed formal analysis and original draft. XFZ was involved in conceptualization.

Declarations

Conflict of interest The authors declare that they have no conflict of interest.

Ethical approval All procedures followed were in accordance with the ethical standards of the responsible committee on human experimentation (Institute of Process Engineering, Chinese Academy of Sciences, China) and with the Helsinki Declaration of 1975, as revised in 2008 (5). Informed consent was obtained from all patients for being included in the study.

References

1. Han XT, Xiao GC, Wang YC et al (2020) Design and fabrication of conductive polymer hydrogels and their applications in flexible supercapacitors. J Mater Chem A 8:23059–23095. https://doi.org/10.1039/D0TA07468C
2. Trung TQ, Ramasundaram S, Hwang BU et al (2016) An all-elastomeric transparent and stretchable temperature sensor for body-attachable wearable electronics. Adv Mater 28:502–509. https://doi.org/10.1002/adma.201504441
3. Peng QY, Chen JS, Wang T et al (2020) Recent advances in designing conductive hydrogels for flexible electronics. InfoMat 2:843–865. https://doi.org/10.1002/inf2.12113
4. Distler T, Boccaccini AR (2020) 3D printing of electrically conductive hydrogels for tissue engineering and biosensors—a review. Acta Biomater 101:1–13. https://doi.org/10.1016/j.actbio.2019.08.044
5. Zhao Y, Li ZH, Li QJ et al (2020) Transparent conductive supramolecular hydrogels with stimuli-responsive properties for on-demand dissolvable diabetic foot wound dressings. Macromol Rapid Commun 41:2000441. https://doi.org/10.1002/marc.202000441
6. Han QQ, Chen Y, Song W et al (2019) Fabrication of agarose hydrogel with patterned silver nanowires for motion sensor. Bio-Design and Manufacturing 2:269–277. https://doi.org/10.1007/s42242-019-00051-w
7. You JO, Auguste DT (2010) Conductive, physiologically responsive hydrogels. Langmuir 26:4607–4612. https://doi.org/10.1021/la100294p
8. Liu XF, Miller AL, Park S et al (2017) Functionalized carbon nanotube and graphene oxide embedded electrically conductive hydrogel synergistically stimulates nerve cell differentiation. ACS Appl Mater Interfaces 9:14677–14690. https://doi.org/10.1021/acsami.7b02072
9. Wang YH, Lv C, Hu RF et al (2020) An all-in-one supercapacitor with high stretchability via a facile strategy. J Mater Chem A 8:8255–8261. https://doi.org/10.1039/d0ta00757a
10. Shi ZQ, Gao HC, Feng J et al (2014) In situ synthesis of robust conductive cellulose/polypyrrole composite aerogels and their potential application in nerve regeneration. Angew Chem Int Ed 53:5380–5384. https://doi.org/10.1002/anie.201402751
11. Pyarasani RD, Jayaramudu T, John A (2019) Polyaniline-based conducting hydrogels. J Mater Sci 54:974–996. https://doi.org/10.1007/s10853-018-2977-x
12. Feig VR, Tran H, Lee M et al (2019) An electrochemical gelation method for patterning conductive PEDOT:PSS hydrogels. Adv Mater 31:1902869. https://doi.org/10.1002/adma.201902869
13. Chen XL, He MM, Zhang XH et al (2020) Metal-free and stretchable conductive hydrogels for high transparent conductive film and flexible strain sensor with high sensitivity. Macromol Chem Phys 221:2000054. https://doi.org/10.1002/macp.202000054
14. Ge G, Zhang YZ, Shao JJ et al (2018) Stretchable, transparent, and self-patterned hydrogel-based pressure sensor for human motions detection. Adv Funct Mater 28:1802576. https://doi.org/10.1002/adfm.201802576
15. Chen R, Xu XB, Yu DF et al (2018) Highly stretchable and fatigue resistant hydrogels with low Young's modulus as transparent and flexible strain sensors. J Mater Chem C 6:11193–11201. https://doi.org/10.1039/c8tc02583e
16. Noshadi I, Walker BW, Portillo-Lara R et al (2017) Engineering biodegradable and biocompatible bio-ionic liquid conjugated hydrogels with tunable conductivity and mechanical properties. Sci Rep 7:4345. https://doi.org/10.1038/s41598-017-04280-w
17. Liang XT, Qu B, Li JR et al (2015) Preparation of cellulose-based conductive hydrogels with ionic liquid. React Funct Polym 86:1–6. https://doi.org/10.1016/j.reactfunctpolym.2014.11.002
18. Han L, Yan LW, Wang MH et al (2018) Transparent, adhesive, and conductive hydrogel for soft bioelectronics based on light-transmitting polydopamine-doped polypyrrole nanofibrils. Chem Mater 30:5561–5572. https://doi.org/10.1021/acs.chemmater.8b01446
19. Johnson KA, Gorzinski SJ, Bodner KM et al (1986) Chronic toxicity and oncogenicity study on acrylamide incorporated in the drinking water of Fischer 344 rats. Toxicol Appl Pharmacol 85:154–168. https://doi.org/10.1016/0041-008x(86)90109-2
20. Parzefall W (2008) Minireview on the toxicity of dietary acrylamide. Food Chem Toxicol 46:1360–1364. https://doi.org/10.1016/j.fct.2007.08.027
21. Yan XH, Zhu PL, Li JB (2010) Self-assembly and application of diphenylalanine-based nanostructures. Chem Soc Rev 39:1877–1890. https://doi.org/10.1039/b915765b
22. Sun BB, Tao K, Jia Y et al (2019) Photoactive properties of supramolecular assembled short peptides. Chem Soc Rev 48:4387–4400. https://doi.org/10.1039/c9cs00085b
23. Wei G, Su ZQ, Reynolds NP et al (2017) Self-assembling peptide and protein amyloids: from structure to tailored function in nanotechnology. Chem Soc Rev 46:4661–4708. https://doi.org/10.1039/c6cs00542j
24. Tao K, Xue B, Li Q et al (2019) Stable and optoelectronic dipeptide assemblies for power harvesting. Mater Today 30:10–16. https://doi.org/10.1016/j.mattod.2019.04.002
25. Yuan CQ, Li SK, Zou QL et al (2017) Multiscale simulations for understanding the evolution and mechanism of hierarchical peptide self-assembly. Phys Chem Chem Phys 19:23614–23631. https://doi.org/10.1039/c7cp01923h

26. Wang MY, Zhang QS, Jian HL et al (2020) Role of thermolysin in catalytic-controlled self-assembly of Fmoc-dipeptides. CCS Chem 2:317–328. https://doi.org/10.31635/ccschem.020.201900116
27. Lampel A, Ulijn RV, Tuttle T (2018) Guiding principles for peptide nanotechnology through directed discovery. Chem Soc Rev 47:3737–3758. https://doi.org/10.1039/c8cs00177d
28. Feng L, Ren P, Hao LN et al (2019) Fabrication of short peptide cages by interfacial self-assembly on $CaCO_3$ templates. Colloids Surf A 573:22–29. https://doi.org/10.1016/j.colsurfa.2019.04.048
29. Wang MY, Wang AH, Li JL et al (2020) Thermolysin-triggered short peptides self-assembly in confined space and application in cell culturing. Colloids Surf A 603:125213. https://doi.org/10.1016/j.colsurfa.2020.125213
30. Ray TR, Choi J, Bandodkar AJ et al (2019) Bio-integrated wearable systems: a comprehensive review. Chem Rev 119:5461–5533. https://doi.org/10.1021/acs.chemrev.8b00573
31. Ye Q, Zhou F, Liu WM (2011) Bioinspired catecholic chemistry for surface modification. Chem Soc Rev 40:4244–4258. https://doi.org/10.1039/c1cs15026j
32. Ryu JH, Messersmith PB, Lee H (2018) Polydopamine surface chemistry: a decade of discovery. ACS Appl Mater Interfaces 10:7523–7540. https://doi.org/10.1021/acsami.7b19865
33. Zhai YG, Duan HD, Meng X et al (2015) Reinforcement effects of inorganic nanoparticles for double-network hydrogels. Macromol Mater Eng 12:1290–1299. https://doi.org/10.1002/mame.201500215
34. Su N, Li HB, Yuan SJ et al (2012) Synthesis and characterization of polypyrrole doped with anionic spherical polyelectrolyte brushes. Express Polym Lett 6:697–705. https://doi.org/10.3144/expresspolymlett.2012.75
35. Akbarian M, Kianpour M, Yousefi R et al (2020) Characterization of insulin cross-seeding: the underlying mechanism reveals seeding and denaturant-induced insulin fibrillation proceeds through structurally similar intermediates. RSC Adv 10:29885–29899. https://doi.org/10.1039/d0ra05414c
36. Soulages JL, Kim K, Walters C et al (2002) Temperature-induced extended helix/random coil transitions in a group 1 late embryogenesis-abundant protein from soybean. Plant Physiol 128:822. https://doi.org/10.1104/pp.010521
37. Wolny M, Batchelor M, Bartlett GJ et al (2017) Characterization of long and stable de novo single alpha-helix domains provides novel insight into their stability. Sci Rep 7:44341. https://doi.org/10.1038/srep44341
38. Ladokhin AS, Selsted ME, White SH (1999) CD spectra of indolicidin antimicrobial peptides suggest turns, not polyproline helix. Biochemistry 38:12313–12319. https://doi.org/10.1021/bi9907936
39. Kenry LB (2018) Recent advances in biodegradable conducting polymers and their biomedical applications. Biomacromol 19:1783–1803. https://doi.org/10.1021/acs.biomac.8b00275